

## Microbicides for HIV/AIDS. 3. Observation of Apparent Dynamic Protonation and Deprotonization in CD4+ T-Cell Model Systems

R. L. Rowell,<sup>‡</sup> D. Fairhurst,<sup>†</sup> I. M. Monahan,<sup>§</sup> S. Key,<sup>§</sup> A. Morfesis,<sup>\*,||</sup> D. Stieh,<sup>§</sup> M. Mitchnick,<sup>⊥</sup> A. Loxley,<sup>⊥</sup> and R. A. Shattock<sup>§</sup>

<sup>†</sup>International Partnership for Microbicides, Silver Spring, Maryland 20910, <sup>‡</sup>Department of Chemistry, University of Massachusetts, Amherst, Massachusetts 01003, <sup>§</sup>St. George's Hospital, University of London, London SW17 0RE, United Kingdom, <sup>||</sup>Malvern Instruments Ltd., Malvern, WR14 1XZ, United Kingdom, and <sup>⊥</sup>Particle Sciences Inc., Bethlehem, Pennsylvania 18017

Received December 4, 2008. Revised Manuscript Received March 30, 2009

New measurements of the electrophoretic mobility of T-cell model systems have been carried out and analyzed to obtain the dynamic variation in mobility in small titration increments during separate upscale and downscale sweeps in pH. We demonstrate that a plot of  $p\lambda$  vs  $p[\text{NaCl}]$  has been found essential in evaluating the consistency of electrophoretic mobility measurements at different (1:1) electrolyte concentrations and show, for the first time, that electrophoretic mobility measurements as a function of pH can reflect different rates of the respective ionization and association that occur in the surface functional groups as a consequence of the different changes in the hydration–dehydration reactions involved. Differences found between the upscale and downscale sweeps suggest that it is easier to protonate a protein cell surface than to deprotonate it. The effect is most pronounced at the highest salt concentration (similar to that which exists for the cells in their native state) and becomes less pronounced as the salt concentration is lowered. The effect is interpreted as a result of the different changes in the state of hydration as a proton moves from the bulk through the double layer to a surface group and the reverse. The effect occurs with both replicating and activated T-cells. This latter result may be of biological significance and particularly relevant to HIV-1 infection, since during male-to-female transmission, the environment where most infections occur supports this protonation effect.

### Introduction

According to the World Health Organization,<sup>1</sup> almost 40 million people were living with HIV at the end of 2004. The epidemic continues with an estimated 2.5 million new infections occurring globally each year.<sup>2</sup> There are no candidate vaccines in the pipeline that can induce sterilizing immunity and protect against infection with HIV-1. Semen-borne virus exists in both cell-free form and within infected leukocytes, but cell-free virus seems to be substantially capable of crossing mucosal surfaces and establishing infection; while cell-associated virions may supply local reservoirs of infectious particles.<sup>3</sup> Targeting intraluminal free virus, or its cellular targets, should be more effective clinically than the complex strategies needed to eliminate virus contained within infected leukocytes in the semen. Therefore, there is a strong clinical need for what have become known as “microbicides”—topically applied agents that prevent vaginal transmission of HIV from person to person.<sup>4</sup> HIV-1 mucosal transmission plays a critical role in HIV-1 infection and AIDS pathogenesis: a recent review has summarized the latest advances in biological studies of HIV-1 mucosal transmission.<sup>5</sup> If the initial virus–cell interaction is inhibited at any stage, then HIV is prevented from entering the target cells.

Our work has been directed at contributing to the solution to this worldwide HIV-1 problem by investigating the surface

chemical properties of both virions and target cells based on the supposition that the interaction between them is “charge-based”. At the heart of the problem is the attack of the AIDS virion on three susceptible T lymphocyte lines. In previous work, we have reported on a detailed examination of the CD4+ T-Cell H9,<sup>6</sup> and we have extended the work to include CD4+ T-Cells C8166 and Molt-4.<sup>7</sup> The strategy has been to characterize the surface chemistry of each CD4+ T-cell line using the methodology of electrophoretic fingerprinting (EF), which is a correlation of the electrophoretic mobility of colloidal particles as a function of pH and  $p\lambda$ , the logarithm of the system conductivity, where the conductivity is expressed in  $\mu\text{S}/\text{cm}$ , since these units give a convenient scale. Our goal is ultimately to obtain direct experimental evidence of the properties of the HIV virion *in situ* building on the knowledge base gathered in this and previous studies on cells. Details of the methodology and results of the T-cell lines are given in the earlier papers.<sup>6,7</sup>

The unit record in data collection is a pH sweep, typically three repeat measurements at every half of a pH unit over the range from pH 3 to 9. Records are collected at several NaCl concentrations, and the data are input and then analyzed using the software program SURFER<sup>8</sup> to prepare a contour map or EF, so-called because early studies gave swirl patterns resembling human fingerprints. Individual records may also be plotted by the SURFER software program giving a graph of the pH sweep or a 2D wireframe.<sup>6</sup>

(1) Joint United Nations Programme on HIV/AIDS & World Health Organization; *AIDS Epidemic Update: 2005*; Geneva, 2005.

(2) UNAIDS; *AIDS Epidemic Update: 2007*; Geneva, 2007.

(3) Sodora, D. L.; Gettle, A.; Miller, C. J.; Marx, P. A. *AIDS Res. Hum. Retroviruses* **1998**, *14*, 119.

(4) Piot, P. *Message on the occasion of World AIDS Day*, 2004, UNAIDS (online).

(5) Wu, Li. *Curr. Opin. HIV AIDS* **2008**, *3*(5), 534.

(6) Rowell, R. L.; Fairhurst, D.; Key, S.; Morfesis, A.; Monahan, I. M.; Mitchnick, M.; Shattock, R. J. *Langmuir* **2005**, *21*, 10165.

(7) Fairhurst, D.; Rowell, R. L.; Monahan, I. M.; Key, S.; Stieh, D.; McNeill-Watson, F.; Morfesis, A.; Mitchnick, M.; Shattock, R. J. *Langmuir* **2007**, *23*, 2680.

(8) Golden Software, Inc., 809 14th St., Golden, CO 80401.

The new results we report here are the findings that the upscale and downscale titrations are quite dissimilar and which we interpret as differences between the protonation and deprotonation reactions of the protein groups of the cell surface; from our earlier work,<sup>6,7</sup> it is clear that the surfaces are strongly zwitterionic. We postulate that these differences can be explained by changes in the hydration state of the hydrogen ion from the free solution state to the bound state on a functional group on the particle surface.

## Experimental Section

In the previous studies, we examined cells in their replicating state. Full experimental details, including a description of the cell lines, are given in those papers.<sup>6,7</sup> In the present work, we have examined cells that have been activated.

**Samples: Activated Cells.** Resting cells remain in a replication competent and viable state, waiting to be primed by a series of events triggered by invading microorganisms of choice. During a true-life infection, the invading bacterium/virus will, generally speaking, be processed by antigen-presenting cells which in turn cause activation of the T-cells by engaging the CD28 molecule and T-cell receptor resulting in expression of different cell surface proteins or in enhanced expression of already existing ones. Activated cells will have enhanced expression of surface receptors, thereby increasing the chance of additional stimulation by the same antigen. This results in increased expression of various chemokines (cytokines, interleukins, tumor necrosis factor, etc.). T-cell activation is a crucial process in the overall mammalian immune response to infection. Essentially, during T-cell activation, native T-cells undergo clonal expansion followed by antigen specification, and different populations acquire the capability to directly kill target cells infected with pathogens or to produce cytokines essential for regulating the immune response. This activation state can be artificially induced in the laboratory by incubation of T-cell cultures with stimulatory molecules.

**Preparation of Samples.** In vitro activation is thought to mimic events that would occur during an *in vivo* infection. The three T-cell lines (H9, Molt 4, and C8166) were grown and maintained in complete RPMI media (containing 10% heat-inactivated fetal calf serum, 2 mM glutamine, 100 IU/mL penicillin, and 100 µg/mL streptomycin) and kept at 37 °C in a humidified 5% CO<sub>2</sub> incubator.

Cells were stimulated by the addition of phorbol 12-myristate 13-acetate (PMA) to a final concentration of 50 ng/mL and phytohemagglutinin (PHA) to a final concentration of 1 µg/mL for 24 h.

PHA and PMA are two compounds that are known to induce enhanced T-cell activation and cytokine production *in vitro*. PHA is a lectin found in plants that is used as a mitogen to trigger cell division in T-lymphocytes. This compound activates T-cells by binding to cell membrane glycoproteins, including the T-cell receptor CD3 complex.<sup>9</sup> PMA is a croton oil-derived tumor promoting agent,<sup>10,11</sup> which again is potent mitogen that stimulates T-cells<sup>12–14</sup> by the direct activation of the enzyme protein kinase C.<sup>15</sup> Protein kinase C is a central component in signaling pathways that regulate numerous cellular processes in the immune response.<sup>16</sup>

- (9) Chilson, O. P.; Kelly-Chilson, A. E. *Eur. J. Immunol.* **1989**, *19*, 389.
- (10) Schmidt, R.; Hecker, E. *Cancer Res.* **1975**, *35*(5), 1375.
- (11) Furstenberger, G.; Berry, D. L.; Sorg, B.; Marks, F. *Proc. Natl. Acad. Sci. U.S.A.* **1981**, *78*(12), 7722.
- (12) Touraine, J. L.; Hadden, J. W.; Touraine, F.; Hadden, E. M.; Estensen, R.; Good, R. A. *J. Exp. Med.* **1977**, *145*, 460.
- (13) Abb, J.; Bayliss, G. J.; Deinhardt, F. *Immunology* **1979**, *122*, 1639.
- (14) Kabelitz, D.; Totterman, T. H.; Gidlung, M.; Nilsson, K.; Wigzell, H. *Cell. Immunol.* **1982**, *70*, 277.
- (15) Saitoh, T.; Dobkins, K. R. *Brain Res.* **1986**, *379*, 196.
- (16) Baier, G. *Immunol. Rev.* **2003**, *92*, 64.

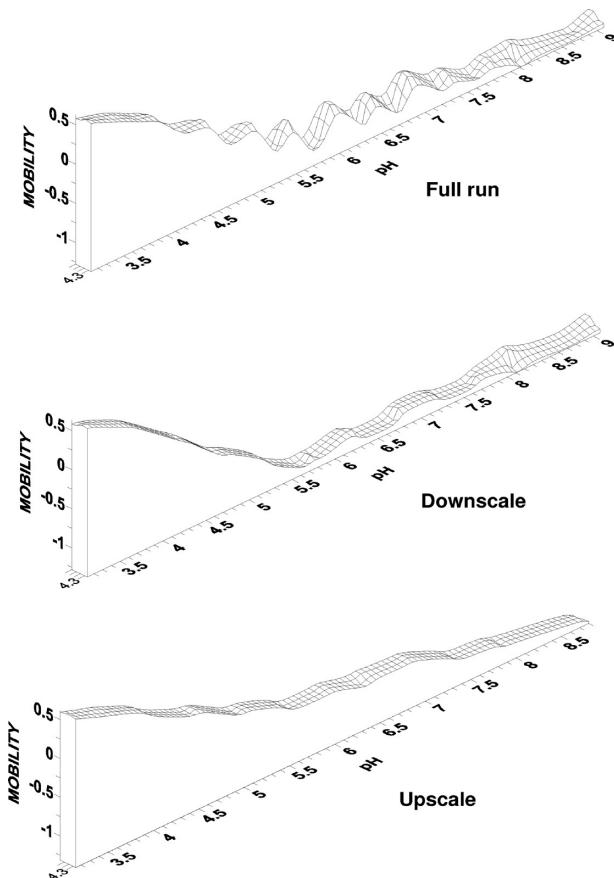


**Figure 1.** 2D wireframes of activated C8166 run 1 in 200 mM NaCl showing the full run (top), the downscale data from pH 9 to pH 3 (middle), and the upscale data from pH 3 to pH 9 (bottom).

**Instrumentation.** Electrophoretic mobility ( $\xi$ -potential) measurements were made using a Malvern ZetaSizer NanoZS operating in the fast field reversal mode (phase analysis light scattering, PALS) equipped with an MPT-2 automatic titrator.<sup>6</sup>

**Data Analysis.** As in previous studies, EXCEL files of raw data were prepared in a format suitable for data analysis using the SURFER software program.<sup>6,7</sup>

## Results for CD4+ T-Cell C8166

**Direction of the pH Sweep.** In Figure 1, we show 2D wireframes of activated C8166 Run1 in 200 mM NaCl. This was the first data from activated samples of the CD4+ T-cells to be analyzed and where directional effects in response to pH changes were first noted. 2D wireframes are a simplified electrokinetic fingerprint (EF) giving the profile dependence of the mobility on pH at a fixed salt concentration. When the salt concentration is the controlling environmental variable, the conductivity of the system is very nearly constant.

The top wireframe shows the full run, which began at pH 8.82 and moved downscale to pH 3.13 then back upscale to pH 8.78. The data were collected over a very narrow range in conductivity from 22.1 to 22.9 mS/cm. The narrow y-axis is  $p\lambda$ , which is the base 10 log of the conductivity expressed in  $\mu\text{S}/\text{cm}$ . For that run, the mean and standard deviation in  $p\lambda$  was  $4.35 \pm 0.004$ . Measurements were sampled in triplicate at intervals of approximately 0.5 pH unit. The ripples in the data (fairly pronounced between approximately pH 5 and 7) were similar to those observed in earlier work.<sup>6</sup> However, in work reported here for the first time, we have discovered that the ripples may largely result from the fact that the downscale data were not sampled at

the same pH values as the upscale data. This is demonstrated in the middle curve which is the downscale data selected from the original run and the lower curve which is from the upscale data from the same run. Both the middle and lower curves are much smoother than the full run.

The ripple effect can be more easily understood through an examination of some of the individual data points. The first triad of the run had measurements at pH values of 8.82, 9.08, and 9.08 with the corresponding mobilities of  $-1.25$ ,  $-1.21$ , and  $-1.13$  with  $p\lambda$  constant at 4.34 to two decimal places. At the lowest pH, the triad gave pH values of 3.12, 3.13, and 3.13 with corresponding mobilities of 0.597, 0.643, and 0.572 and  $p\lambda$  values of 4.37, 4.35, and 4.35 so that individual triads were reasonably self-consistent and the variation in  $p\lambda$  over the sweep was small. However, as shown in Figure 1, the shapes of the downscale and upscale wireframes are quite different.

The ZetaSizer instrument was programmed to make measurements at differences in pH of 0.5, which in practice varied from 0.4 to 0.6 with a single increment at the end of the run of 0.9. However, as the pH change is reversed, it was discovered that the measurements did not fall within the same registration. Consider the midrange region in the top wireframe between pH 5.3 and 6.4 where the ripples are most pronounced. The averaged triad measurements in this range occurred at pH values of 5.3, 5.5, 5.7, 5.9, 6.3, and 6.4 with the corresponding mobilities of  $-1.0$ ,  $-0.6$ ,  $-1.2$ ,  $-0.6$ ,  $-1.2$ , and  $-0.7$ . The downscale set came from the pH values of 5.3, 5.7, and 6.3 with the upscale set of pH 5.5, 5.9 and 6.4. It is apparent that the system reacts differently to the pH gradient in the downscale sweep than in the upscale sweep.

In the downscale sweep, as we add acid, hydrated protons are being added to the external medium, and these have to cross the double layer to combine with carboxyl ions on the cell surface to reduce the negative charge on the protein coat. The hydration state of the proton in the external medium is expected to be different from the hydration state of the proton that has crossed the double layer and combined with a carboxyl anion on the particle surface. As the carboxyl ions are being neutralized at low pH values, hydrated protons also cross the double layer to combine with amino family groups which are also on the zwitterionic surface. It is clear that the processes overlap, but we do not know the exact pH where the amino family groups begin to display positive charge.

This new effect, shown in Figure 1, has been found in numerous runs. The downscale mobility values vary little until pH 5.5 where they turn sharply positive as the lowest pH is approached. Conversely, the upscale sweep shows a more gradual change in mobility toward increasingly negative values as the pH is increased. In our previous work,<sup>6,7</sup> we had assumed that the principal surface group giving rise to the negative charge is the carboxyl group in the cell protein envelope. We have confirmed this by digesting off H9 cell protein using an enzyme (protease) treatment;<sup>17</sup> the subsequent measured EF showed no evidence of a line of zero mobility (LZM) and no pronounced difference between upscale and downscale runs.<sup>18</sup> The positively charged surface groups are more complicated, as we have discussed in our previous paper.<sup>7</sup> Though we are less confident about the exact source, or sources, of positive charge, it is clear that there are different kinds of positive and negative groups that are undergoing independent protonization and deprotonization as we move downscale and upscale in pH. The data suggest that, as

(17) Narahashi, Y. In *Methods in Enzymology*; Perlmann, G. E., Loland, L., Eds.; Academic Press: New York, 1970; Vol 19, p 651.

(18) Unpublished results.

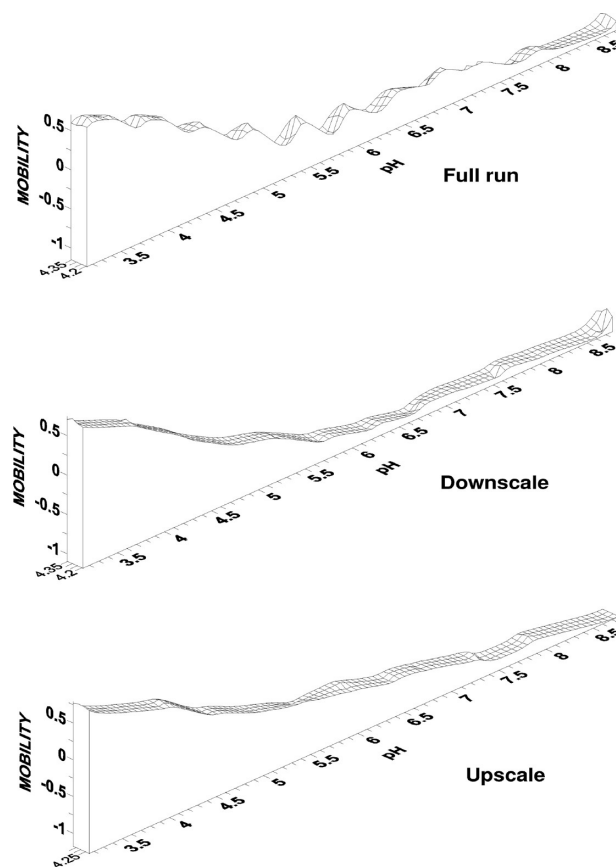


**Figure 2.** 2D wireframes of activated C8166 run 1 in 154 mM NaCl showing the full run (top), the downscale data from pH 9 to pH 3 (middle), and the upscale data from pH 3 to pH 9 (bottom).

the pH is increased, protons move from the particle surface through the double layer and into the ionic environment. The slopes downscale and upscale are dissimilar because different processes, such as changes in proton hydration, are involved when the electric double layer is crossed in different directions by those hydrated protons.

The effect is demonstrated to persist, but to a changing degree, as the measurements are taken at the lower concentrations of 154, 50, and 10 mM NaCl as shown in Figures 2, 3, and 4, respectively. We have found the same effects and trends in numerous other samples of C8166, and also H9 and Molt 4 T-Cell samples, as will be discussed below.

In the downscale, the run begins by first titrating to the maximum pH, and this results in the maximum ionization of the carboxyl groups shown in the middle scans of Figures 2, 3, and 4; note that the maximum mobility scale increases from  $-1.1$  to  $-2.5$  units as the NaCl concentration is decreased from 154 mM down to 10 mM. Conversely, the upscale sweep begins by first titrating to the minimum pH where the cell surface achieves the maximum positive charge (the lower scans of Figures 2, 3, and 4); here, the maximum positive mobility scale increases from  $+0.7$  to  $+1.4$  units as the NaCl concentration is decreased.

The effect is seen to persist at 5 mM NaCl (Figure 5) and even in DI water (Figure 6). In the latter case, the NaCl was nominally zero, but a measurable conductance was detected implying that some ionic environment may have been carried over from the sampling procedure or it may have been osmotically induced from the colloid (T-cell) itself. Generally, a pH titration sweep (up or down) takes about 1.5 h. Microscopic examination indicated that in DI water only 5% of the cells were viable after 1 h—mostly only

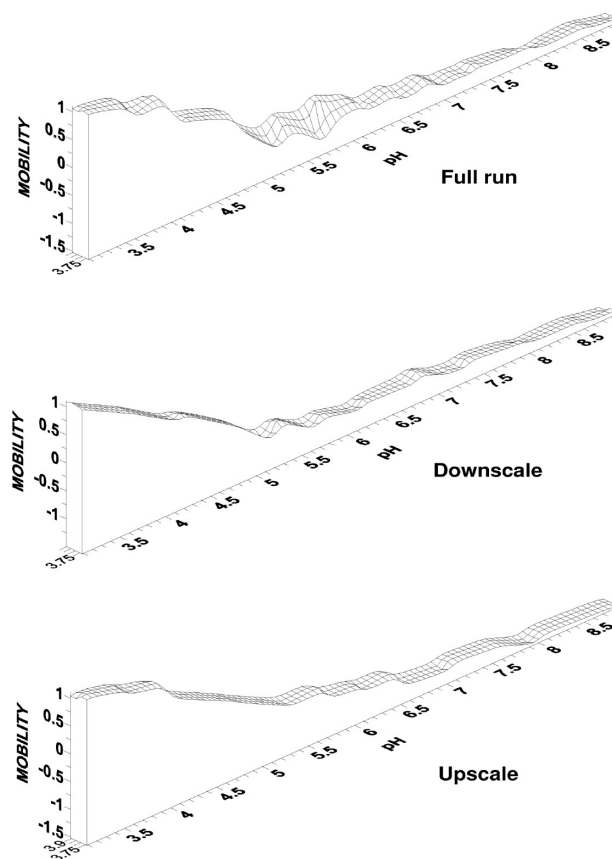


**Figure 3.** 2D Wireframes of activated C8166 run 1 in 50 mM NaCl showing the full run (top), the downscale data from pH 9 to pH 3 (middle), and the upscale data from pH 3 to pH 9 (bottom).

cells debris was visible, implying that the cells had lysed via osmosis—and at 2 h only cell debris was evident. Overall, it appears that the “up/down effect” (discussed below) diminishes in intensity as the salt concentration decreases from 200 mM to 5 mM NaCl. However, as the salt concentration decreases, the overall mobility becomes much more negative owing to expansion of the double layer and deshielding of the surface charge.

In our first paper,<sup>6</sup> we noted the dissimilarity of downsweeps and upsweeps and described it as a hysteresis. From the results presented here, we now suggest that the effects are possibly a consequence of differences in the protonation and deprotonation rates.

**Initial Slopes and Divergence.** Detailed plots of the measured data show that the initial slope of the mobility–pH scans is nearly identical for NaCl concentrations of 200 and 154 mM with the value of  $-0.6$  mobility unit per pH unit. The divergence between the upscale and downscale sweeps becomes pronounced at about pH 4 and increases with increasing pH as shown in Figures 1–6. The initial slope is sharper at the lower NaCl concentrations of 50 and 10 mM with the value of  $-0.9$  to  $-1.0$  mobility units per pH unit. The greater sensitivity to initial slope at the lower NaCl concentrations reflects the increased expansion of the double layer.

The difference in slope between the upscale and downscale sweeps suggests that it is easier to protonate the cell surface functional groups with changing pH than to deprotonate them. In the low pH region, it is largely positively charged groups that are being deprotonated with increasing pH, while in the higher pH region, it is largely the carboxyl groups that are being deprotonated with increasing pH. The slopes in the low pH region are larger than the slopes in the higher pH region, suggesting a

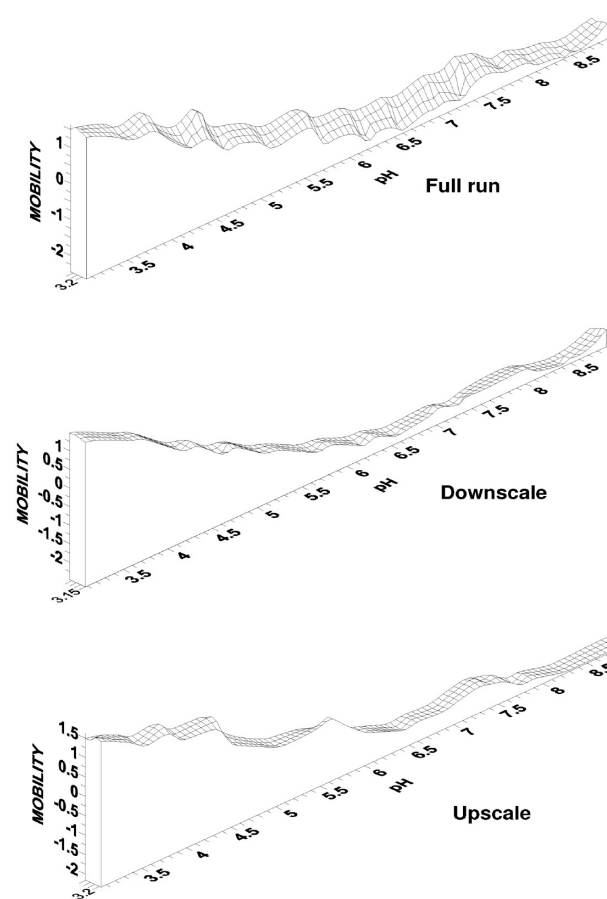


**Figure 4.** 2D Wireframes of activated C8166 Run 1 in 10 mM NaCl showing the full run (top), the downscale data from pH 9 to pH 3 (middle) and the upscale data from pH 3 to pH 9 (bottom).

real distinction between the ionization of positive and negative groups. While our data are not sensitive enough to show molecular detail, it is reasonable to suggest that this diversity arises from differences in the detailed hydration–dehydration processes involved as the protons pass through the double layer.

An overall examination of the results reinforces the preceding ideas:

- 1 The initial point of a sweep determines the state of the system. At high pH, the carboxyl groups are as fully ionized as the existing pH and ionic strength allow. The amino family groups are fully deprotonated.
- 2 At low pH, the carboxyl groups approach complete deprotonation. The amino family groups reach maximum protonation allowed by the existing pH and ionic strength.
- 3 The maximum mobility obtained in Figure 1, 200 mM NaCl, is  $-1.25$ . The maximum mobility obtained in DI water in Figure 6 exceeds  $-2.25$ . Thus, the mobility nearly doubles over the range of salt concentration examined. This masking of the surface charge with increased salt concentration was independent of the direction of titration and reflects the ease at which hydrated protons can cross the double layer.
- 4 In the downsweeps, the negative mobility persists until slightly beyond pH 7, on the acid side of neutrality. The loss of negative mobility occurs in the pH region 5.5–7.5, depending on the NaCl concentration. The loss of negative mobility is interpreted as protonation

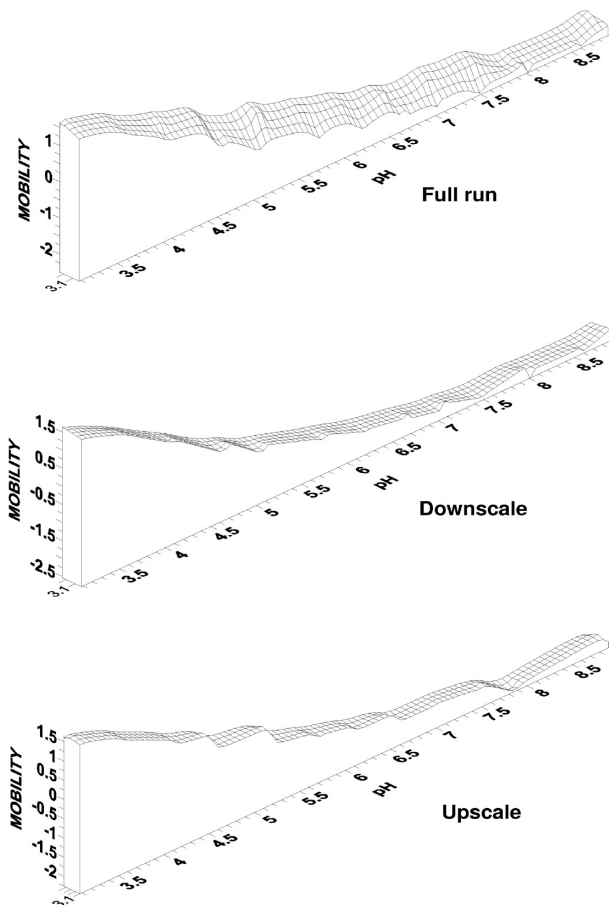


**Figure 5.** 2D wireframes of activated C8166 run 1 in 5 mM NaCl showing the full run (top), the downscale data from pH 9 to pH 3 (middle), and the upscale data from pH 3 to pH 9 (bottom).

of the surface carboxyl ions, and potentially free amines, that compose the protein coat.

- 5 Both downsweep and upsweep display the same mobility of approximately +0.55 at low pH as shown in Figure 1, but the upsweep requires the full pH scan to achieve the maximum mobility of -1.25. This supports the idea that it is more difficult to remove protons from surface groups and transmit them through the interface to enter the bulk solution. This effect slowly changes as the NaCl concentration is decreased so that in Figures 5 and 6 at 5 mM NaCl and DI water, respectively, the profiles of the downsweep and upsweep become more similar.
- 6 Figure 2 for 154 mM NaCl, the physiological condition, shows that on the upsweep maximum mobility allowed by the existing pH and ionic strength is approached around pH 8, on the alkaline side of neutrality.

**Zwitterionic Behavior.** In colloid science, a zwitterionic surface is a surface in which a functional group is present that can exhibit both positive and negative charge, or two groups are present on the surface, one of which is positively charged and the other negatively charged. In the biochemistry of surfaces, the most common type of zwitterionic character comes from the  $\alpha$ -amino acids where the two groups are on neighboring carbon atoms. In that case, one might expect some linkage between the proton exchange between carboxyl and neighboring  $\alpha$ -amino groups. In the large glycoprotein covering the cell surface,

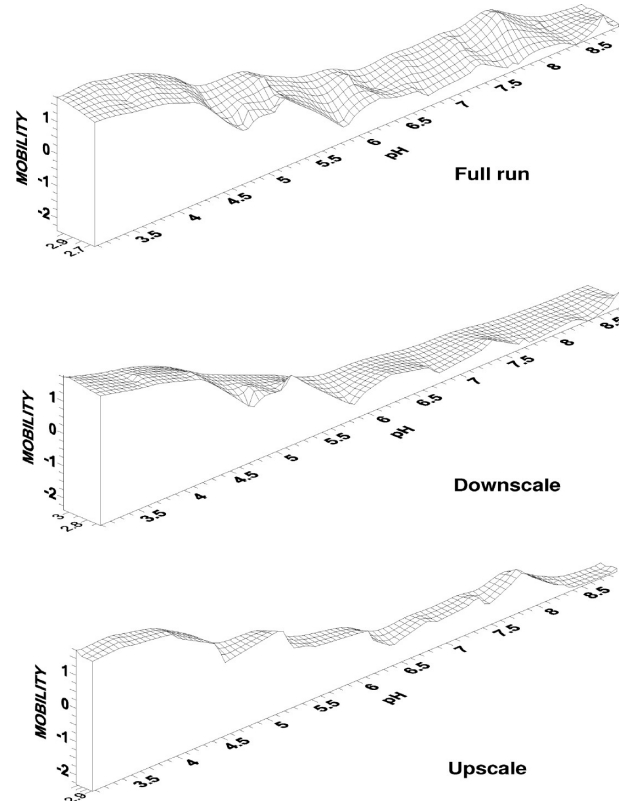


**Figure 6.** 2D wireframes of activated C8166 run 1 in DI water showing the full run (top), the downscale data from pH 9 to pH 3 (middle), and the upscale data from pH 3 to pH 9 (bottom).

it would appear from the high positive mobilities attained that there are more than terminal  $\alpha$ -amino acids contributing to the positive charge indicating that the positive and negative groups on the cell surface would likely be at sufficient separation to act independently. However, we also cannot preclude the possibility that there could be interaction between groups on the cell surface.

**Effect of NaCl Concentration on Double-Layer Expansion.** Marlow<sup>19</sup> showed that a plot of log conductivity vs log KCl should be a straight line. We would expect the same outcome for NaCl.

Figure 7 shows the mean  $p\lambda$  for the full run (filled circles), the downscale sweep (open circles), and the upscale sweep (open triangles) for all of the data collected for a sample of the activated C8166: three points that overlap and are represented by a single filled circle. A good straight line is obtained from 200 mM NaCl down to 10 mM NaCl, and this is the data reported above in Figures 2, 3, and 4. The measurements at 10 mM NaCl and higher are so close it is difficult to show error bars. For example, the mean and standard deviation in  $p\lambda$  at 10 mM NaCl are  $3.24 \pm 0.03$ ,  $3.21 \pm 0.02$ , and  $3.27 \pm 0.01$  for the full run, the downscale sweep, and the upscale sweep, respectively. Below 10 mM NaCl, the double-layer expansion is great and the amount of NaCl added to the sample becomes comparable to the residual electrolyte coming from the particle so that the model of a particle with a double-layer under the influence of a controllable electrolyte environment does not hold. Overall, it appears that plotting  $p\lambda$  vs  $p[\text{NaCl}]$  is a useful procedure in evaluating the consistency of the data.

**Activated C8166 Electrophoretic Fingerprints.** The data that were used to prepare Figures 1–4 were subsequently used to

(19) Marlow, B. J.; Rowell, R. L. *Langmuir* 1991, 7, 2970.

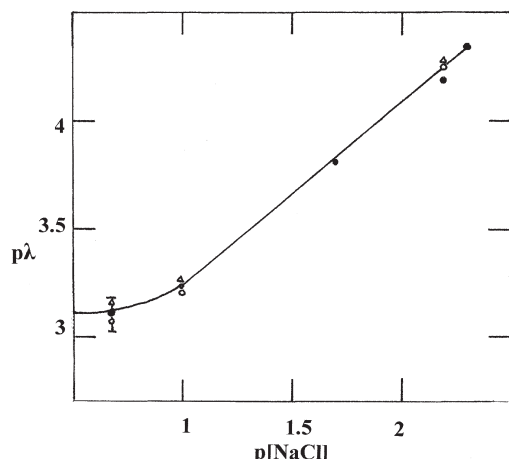


**Figure 7.** Plot of  $p\lambda$  vs  $p[\text{NaCl}]$  for C8166-ac1.  $p\lambda$  is the log of the conductivity in  $\mu\text{S}/\text{cm}$  and  $p[\text{NaCl}]$  is the log of the NaCl concentration in millimolarity. Physiological saline, i.e. 154 mM NaCl, has a  $p\lambda$  value 4.26. The NaCl concentrations are 5, 10, 50, 154, and 200 mM. Symbols are: full run (full circles), downscale (open circles), and upscale (open triangles). Three points that overlap are shown as a filled circle.

construct electrophoretic fingerprints (EFs) for activated C8166 (Figure 8). The upscale EF (lower scan of Figure 8) shows a more positive mobility than the downscale EF. The region to the left of the LZM is larger, and indeed, the entire LZM has shifted approximately a quarter of a pH unit toward higher pH.

The results suggest that a small change in pH near the LZM may affect the balance of charge on the particle surface. This is potentially of biological significance, for example, if an approaching viral cell brought an accompanying change in the local pH as it approached a target T-cell. It is known that the pH values of vaginal and seminal fluids are quite different.<sup>20,21</sup> In healthy women, the pH of vaginal fluid is mildly acidic (pH range: >4 to <6.5). Indeed, OTC women's personal products such as Buffer Gel<sup>22</sup> are designed to maintain vaginal acidity. The pH of seminal fluid is mildly alkaline (pH range >7 to ca. 8.5) and also has a greater buffer capacity. Thus, during male-to-female intercourse—the point at which HIV is introduced—the pH environment in the vaginal lumens increases rapidly.

Figures 9 and 10 show two EFs obtained from a further five runs on each of two additional samples of activated C-8166; these are almost identical in the path traced by the LZM with very similar charge distributions. The isoelectric points (iep), taken as the intersection of the LZM with the lowest  $p\lambda$  coordinate axis, for the downscale sweeps agree (4.5) but differ from the upscale ieps (5.3), which also agree with each other. However, they differ significantly from the EF pattern in Figure 8. The principal differences are seen in the data at the lower NaCl concentrations of 10 and 50 mM. All three sets at 10 mM were run on the same day, and all three sets on the 50 mM were also run on the same day but about one week later. A possible reason for the observed disagreement might lie in the activation process or number of times that the cells had been passaged prior to activation. Although all the experiments were carried out on different days, great care was taken to ensure that everything was as reproducible as possible. However, the C8166 T-cell line grows as large clumps of replicating cells, compared to the other two cell lines under

(20) Katz, D. F.; Anderson, M. H.; Owen, D. H.; Plenys, A. M.; Walmer, D. K. In *Vaginal Microbicide Formulations Workshop*; Rencher, W. F., Ed.; Lippincott-Raven Publishers: Philadelphia, 1998.

(21) Katz, D. F.; Owen, D. H. *Contraception* 1999, 59, 91.

(22) ReProtect, Inc., Baltimore, MD 21286, USA; www.reprotect.com.

investigation (Figure 11).<sup>23</sup> The trend is, however, the same for the three data sets, viz. the upscale iep is shifted to a higher pH value compared to the downscale.

#### Comparison with Previous Work on Replicating C8166.

Figure 12 shows downscale and upscale EFs for replicating C8166. The overall patterns bear some resemblance to the activated C8166, but LZMs differ. The difference in up/down "ieps" is smaller (ca. 0.2 pH units). The replicating EFs look more "uniform" than their activated siblings. However, this may just be a simple consequence of the number of runs analyzed.

Cell lines are inherently activated by their immortality; hence, the nature of a cell line is that it cannot enter a quiescent or "resting" state since it is constantly dividing (replicating). Thus, such cell lines are not truly "inactive". True resting cells are represented by primary cells that have been isolated and untreated. Primary cells require external activation in order to be susceptible to infection, while cell lines, like C8166, are biologically always at the same elevated state in activation; they are susceptible to infection even without PHA/PMA induced activation. Stimulating the C8166 with PHA/PMA results in a more highly activated state, and this is mirrored by changes in surface chemical profile as a function of pH.

#### Results for CD4 + T-Cell H9

**Previous Work.** The electrophoretic fingerprints of replicating H9 cells have been reported in two previous publications,<sup>6,7</sup> and we were unaware of the deprotonization–protonization effect at that time. It is convenient to refer to the deprotonization–protonization effect as the up–down effect, since deprotonization occurs going upscale from low to high pH while protonization occurs on the downswing, the reverse, or the acidification sweep from high to low pH.

Throughout the progression of our work, different protocols were used in the accumulation of the data. The initial protocol was to start at the pH dictated by the growth medium, which was in the mid-pH range and sweep up to a maximum pH around 8 or 9, then return downscale to a minimum around pH 3. Other protocols that were used were as follows: (i) titrate immediately to the highest pH, sweep to the lowest pH, and return upscale to the highest pH; and (ii) titrate immediately to the lowest pH and sweep upscale to the highest pH, then a full return downscale to the beginning. We were not aware of the dynamics of the sweeps nor any possible long-term equilibration effects that might occur. These and other insights have now caused us to reexamine the earlier data on replicating H9 and to add new data on activated H9. For whatever protocol was followed, it has been possible to separate the collected data into individual up- and downsweeps.

**Replicating H9.** In Figure 13, we have separated the previous data<sup>6,7</sup> to show the fingerprints for the full run, the downswing, and the upswing. The EFs for the downswing and the upswing are clearly quite different. The downswing retains the LZM loop that appeared in the original full run, but also a new LZM spot is evident; neither the loop nor the spot is evident in the upswing data.

In our first paper<sup>6</sup> we had postulated that the LZM loop might have been an artifact arising from the statistical analysis of the SURFER program. Accordingly, it was decided to check the linearity of a plot of  $p\lambda$  vs  $p[\text{NaCl}]$  for all of the previous H9 data. The plot, shown in Figure 14, brings to light that seven runs did not fall on the line: three runs at 200 mM NaCl, three runs at 10 mM NaCl, and one run at 1 mM NaCl. Accordingly, new EFs

(23) Salahuddin, S. Z.; Markham, P. D.; Wong-Stall, F.; Franchini, G.; Kalyanaraman, V. S.; Gallo, R. C. *Virology* 1983, 129, 51.

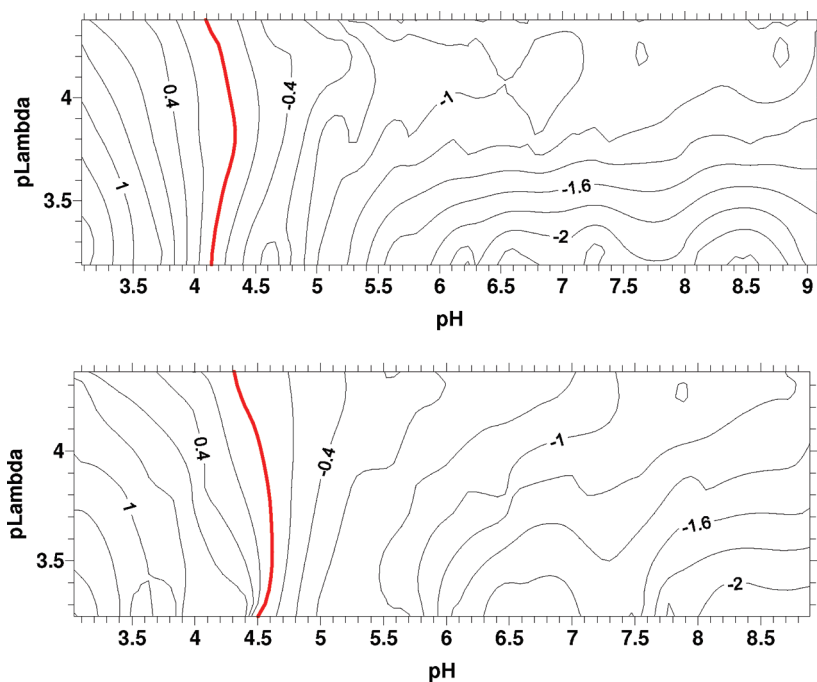


**Figure 8.** Electrophoretic fingerprints of activated C8166 run 1 prepared from downscale (top) and upscale (bottom) data at 10, 50, 154, and 200 mM NaCl.

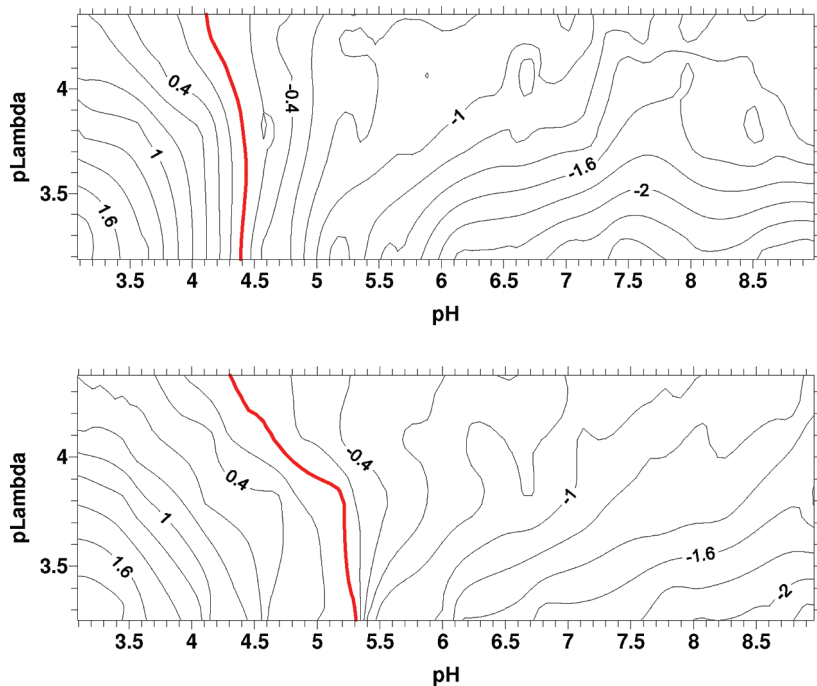


**Figure 9.** Electrophoretic fingerprints of activated C8166 run 2 prepared from downscale (top) and upscale (bottom) data at 10, 50, 100, 154, and 200 mM NaCl.

were constructed using only the nine runs that fell on the line in Figure 14. From the results shown in Figure 15, it is now apparent that the LZM loop and spot in the original EF were, indeed, artifacts. The difference in up/down “ieps” is again small (ca. 0.2 pH units).

It is difficult to make a quantitative comparison between replicating H9 in Figure 15 and resting C8166 in Figure 12 because quite different amounts of data were used, resulting in the apparent diverse complexity. However, the approximate iep (discussed below) of C8166 is shifted to higher pH with respect to H9 in both the upsweep and the downsweep.

**Activated H9.** Given all the foregoing, a comprehensive investigation of activated H9 data was carried out. Three sets of data, each ranging from 200 mM to 5 mM NaCl, gave 18 runs that all fell on a good straight line in a plot of  $p\lambda$  vs  $p[\text{NaCl}]$  (not shown). Thus, it was concluded that all the data could be used to construct EFs, and these are shown in Figure 16. The difference in up/down “ieps” is the same as for the replicating cells (ca. 0.2 pH units), but the ieps for the activated cells are shifted to higher pH. In addition, similarly to C8166, stimulation of the H9 cells seems to provoke a change in surface chemical profile.

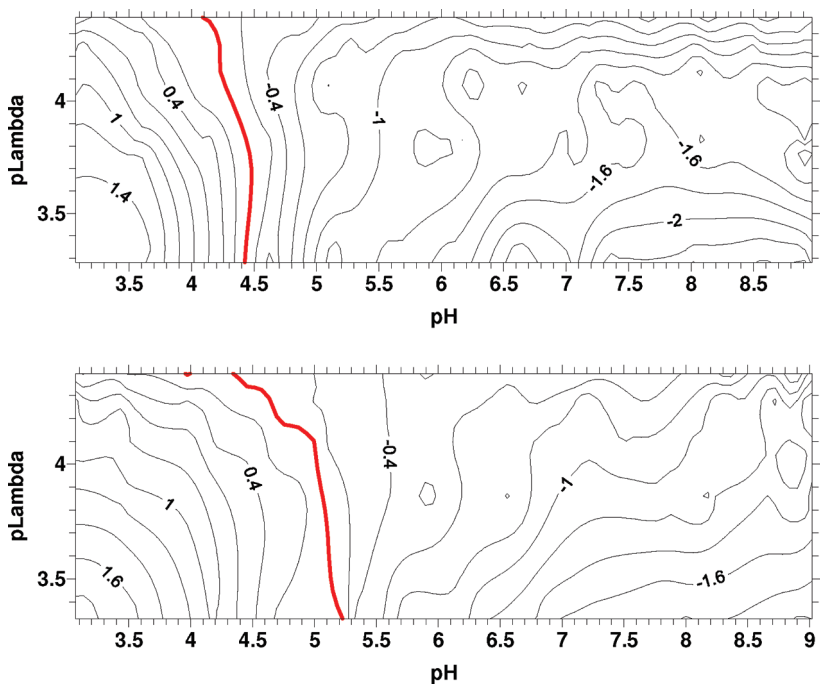


**Figure 10.** Electrophoretic fingerprints of activated C8166 run 3 prepared from downscale (top) and upscale (bottom) data at 10, 50, 100, 154, and 200 mM NaCl.

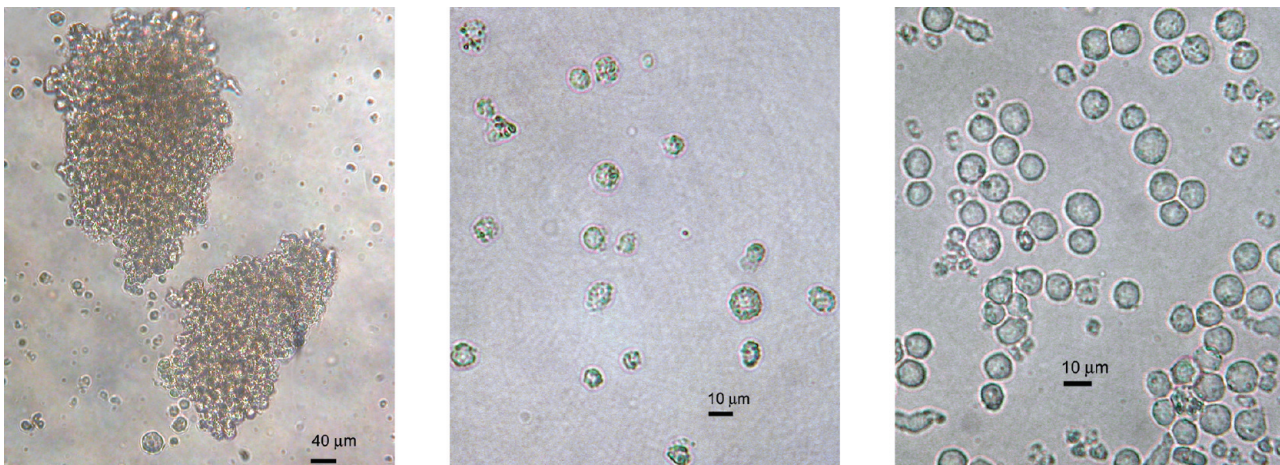


**Figure 11.** Optical microscopic images (mag 400 $\times$ ) of replicating T-cell lines: (a) C8166, (b) H9, and (c) Molt 4.

### Results for CD + T-Cell Molt 4

**Replicating Molt 4.** The previous work on Molt 4<sup>6</sup> was reviewed, and again using a plot of  $p\lambda$  vs  $p[\text{NaCl}]$  to evaluate data consistency, it was found that two runs, taken at 0.5 mM and 1 mM NaCl, did not fall on the straight line. The data of the full run were also separated into downscale and upscale sweeps as shown in Figure 17. A ripple effect, again arising from the difference between the upsweeps and the downsweeps and similar to that for the two other cell lines, was found for Molt 4 (not shown). The difference in the downscale and upscale LZMs for Molt 4 was most apparent at very high and very low  $p\lambda$  where the upscale sweep was shifted toward higher pH, as was the case with the other cell lines. Over  $p\lambda$  3.3 to 4, the LZMs followed a very similar path.

**Activated Molt 4.** A total of sixteen data files were analyzed. These comprised one run of five files and two runs of eleven files; the second set of additional data was obtained almost a year later. There appeared to be a small individual differentiation among the

files, but they were close enough in our judgment to allow analysis of the whole group. The mean  $p\lambda$  of one file was significantly removed from the straight line on a plot of  $p\lambda$  vs  $p[\text{NaCl}]$  (not shown) for all files and so it was rejected. The individual 2D wireframes at a given salt concentration also showed the ripple effect (not shown). The iep for the upsweep was at slightly higher pH than the that for the downsweep (Figure 18). A loop and a point LZM shown in the 154–200 mM NaCl region around pH 4 in the upscale data appears to be a curve-fitting artifact arising from the very low mobilities in that region.

A comparison of the EFs between resting and activated Molt 4 (Figures 17 and 18) shows that the ieps for the activated Molt 4 were again shifted toward higher pH. Furthermore, the maximum positive and maximum negative mobilities for the activated Molt 4 were significantly less than the corresponding values for the resting sibling cells. Thus, unlike both the C8166 and H9 cell lines, stimulation of the Molt 4 results in a smaller change in surface chemical profile.

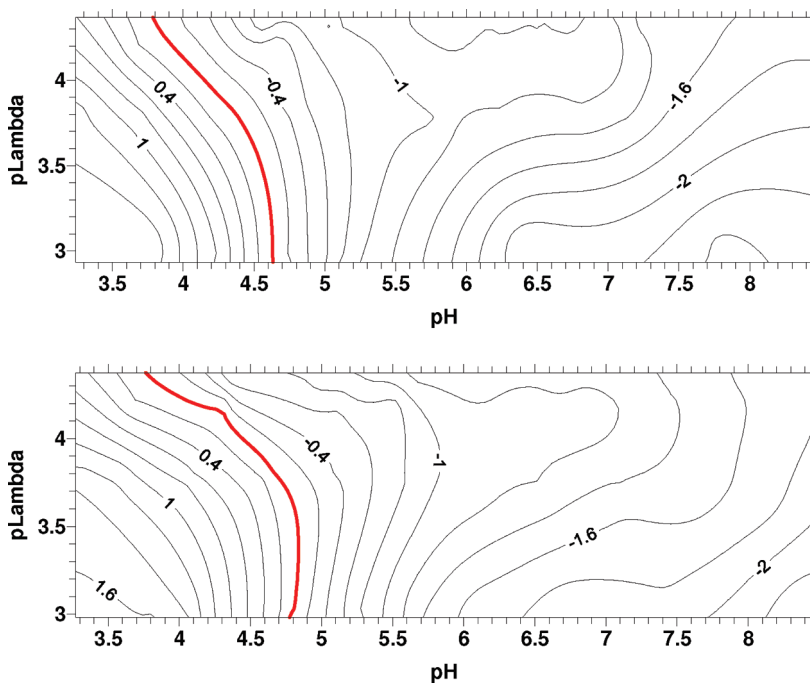


**Figure 12.** Electrophoretic fingerprints of replicating C8166 prepared from downscale (top) and upscale (bottom) data at 5, 50, 154, and 200 mM NaCl.

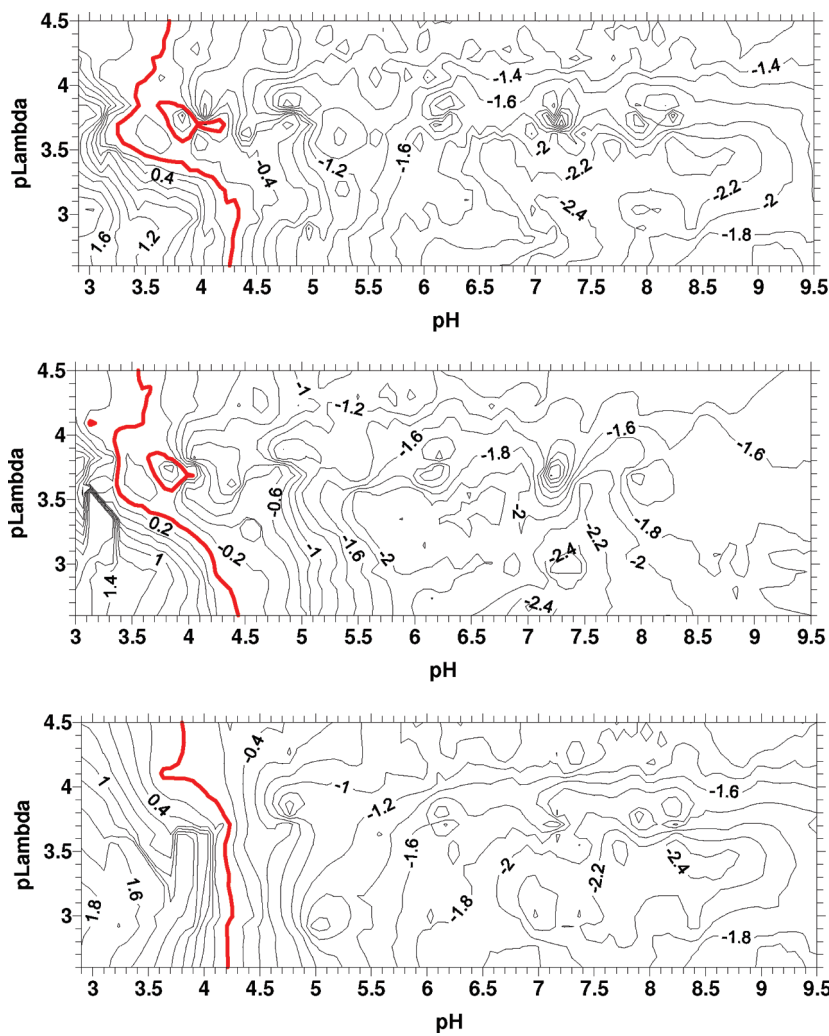


**Figure 13.** Electrophoretic fingerprints of replicating H9: top, full run; middle, downsweep (pH 9.5 to pH 3); and bottom, upsweep (pH 3 to pH 9.5).

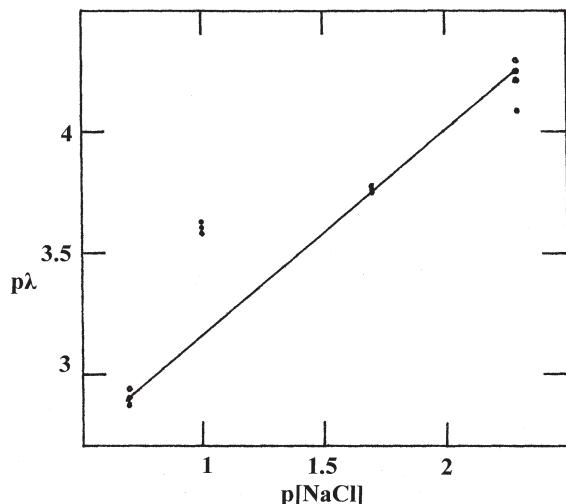


**Figure 14.** Plot of  $p\lambda$  vs  $p[\text{NaCl}]$  for all of the data for H9 files used in the preparation of previous *Langmuir* papers. The NaCl concentrations are 5, 10, 50, and 200 mM.

## Discussion

**Electrophoretic Fingerprints.** From our results, we can make a number of general statements:

- 1 All EFs, for all of the systems measured, differ according to whether the data were taken by upscale or downscale scans in pH. This is true for each of the different data collection protocols used. In general, three different protocols were used: (i) Begin at the pH of the aliquot selected, which is generally nearly neutral, and then measure to the highest pH desired; sweep downscale to the lowest pH desired; sweep upscale to the initial pH. (ii) Titrate to the highest pH desired and measure in a downswEEP to the lowest pH desired followed directly by an upswEEP measurement to the highest pH. (iii) Titrate to the lowest pH desired and measure in an upswEEP to the highest pH desired, followed immediately by a downswEEP measurement to the lowest pH. Consistent results are obtained when the data are separated into upswEEP and downswEEP directions for analysis, no matter which data collection protocol was used. Subsequent analysis and fingerprint plotting should reflect a unified methodology.
- 2 Three cell lines, each in replicating and activated states, with individual upscale and downscale EFs gave twelve independent characteristic fingerprints.
- 3 Minor changes in the characteristics of the fingerprints could be seen with different samples. Where this had significance in LZM shifts and general level of charge, additional EFs have been shown, rather than to collect all data for an “average” fingerprint.
- 4 The LZMs at the lowest  $p\lambda$ s measured may be taken as an approximation for the isoelectric point of the system.
- 5 The LZMs at the highest  $p\lambda$ s measured show some remarkable differences in the EFs reported; this probably arises from differences in the up-down kinetics when the double layer is under severe compression at such high salt concentration. However, this concentration is more indicative of the native state of the cells. Measurements at equilibrium, instead of titration, should allow more accurate placement of zero mobility regions.

- 6 The EF is only as valid as the data that are selected to prepare the EF. In the H9 system, Figures 13–16, we demonstrate, for the first time, how the  $p\lambda$ – $p[\text{NaCl}]$  plot may be used to detect inconsistent data, and we have applied it to all further cell data.

**Isoelectric Points.** For each EF, the intersection of the LZM with the lowest  $p\lambda$  coordinate measured may be taken as an approximation to the isoelectric point (iep) for each cell line. The ieps, so determined for all of the EFs reported, are summarized in Table 1. It has to be recognized that the current measurements are nonequilibrium. Such differences observed in the EFs might disappear if the system is left to attain a true equilibrium. Among the replicating cells, the C8166 line has a significantly higher value than either H9 and Molt 4. For all three cell lines, stimulation with PHA/PMA results in a measurable change in surface chemical profile. As a class, among the activated cells with the exception of the downscale activated C8166, their ieps are generally higher than those for the replicating cells. Indeed, two of the activated C8166 samples have the highest ieps in the table. With the exception of replicating H9, all of the upscale ieps are higher than the downscale ieps.

**2D Wireframes.** As mentioned earlier, the 2D Wireframes reported in Figures 1–6 are actually EFs measured over a very small range in  $p\lambda$  as long as the linear relation holds on the  $p\lambda$ – $p[\text{NaCl}]$  plot. At very low salt concentration, where the  $p\lambda$ – $p[\text{NaCl}]$  plot becomes nonlinear, the  $p\lambda$  range broadens as the system is controlled by the residual electrolyte surrounding the particle as well as the conductivity of the particles themselves.

The difference in the downscale and upscale sweeps in the 2D wireframes shown gives rise to a simple interpretation of the data: Deprotonation occurs over a relatively long range in pH, suggesting that a large pH gradient is needed to remove the (hydrated) protons from surface functional groups through the double layer and into the bulk of the electrolyte. Protonation occurs rather slowly on the downswEEP over a long range in pH, but in the lower pH region, it undergoes a rapid change that is determined by both the neutralization of carboxyl ions and the protonation of the nitrogenous groups on the particle surface. Comparing the protonation and deprotonation processes leads to the suggestion that free hydrated hydrogen ions can more readily cross the double layer onto the particle surface than the bound hydrated hydrogen ions can leave the particle surface and cross the double layer to enter the bulk medium.

## Comparison with Other Studies

**Isoelectric Points.** Homola<sup>24</sup> studied amphoteric polystyrene latices with well-defined carboxyl and amino groups as model systems. The latices were polymerized from *N,N*-diethylaminoethyl methacrylate and methacrylic acid. For a recipe with no methacrylic acid, the iep was pH 8, and it shifted to lower pH with increasing carboxyl groups. At an acid-to-amine ratio of 5.47, the iep was at pH 4.2. Harding<sup>25</sup> worked with purified amphoteric latices and reported ieps ranging from pH 5.4 to 8. Valle-Delgado<sup>26</sup> also studied amphoteric latex and reported an iep at pH 6 in 2 mM NaCl, which shifted to pH 4 in 500 mM NaNO<sub>3</sub>. Musyanovych<sup>27</sup> prepared nanoparticles in a two-step process where the first step produced carboxyl groups on the polystyrene latex surface and the second step grafted amino-functional

(24) Homola, A.; James, R. O. *J. Colloid Interface Sci.* **1977**, *59*, 123.

(25) Harding, I. H.; Healy, T. W. *J. Colloid Interface Sci.* **1982**, *89*, 185.

(26) Valle-Delgado, J. J.; Molina-Bolívar, J. A.; Galisteo-Gonzalez, F.; Galvez-Ruiz, M. *J. Colloid Polym. Sci.* **2003**, *281*, 708.

(27) Musyanovych, A.; Adler, H.-J. P., *Langmuir* **2005**, *21*, 2209.

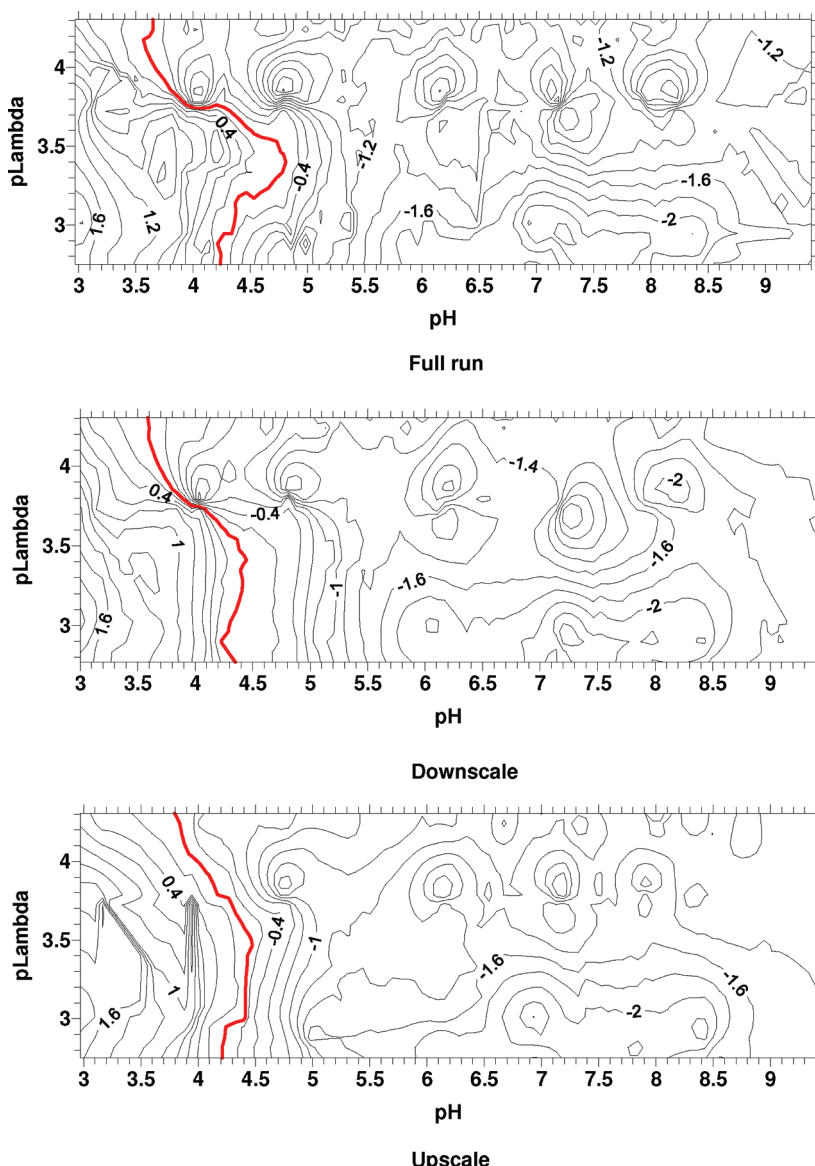


**Figure 15.** Electrophoretic fingerprints of replicating H9: Top, full run; middle, downsweep (pH 9 to pH 3); and bottom, upsweep (pH 3 to pH 9) prepared from the data runs on the line in Figure 13.

monomer onto the surface; an iep at pH 4 was found in 1 mM KCl. Dufrene<sup>28</sup> studied biological colloid aminocarboxyl brewer's yeast cells, *S. cerevisiae*, and reported an iep at pH 4. Thus, all of the preceding papers report ieps that are consistent with the ieps reported in Table 1.

We ourselves have carried out a study of two PS latexes—one carboxylic and the second zwitterionic—looking at both upscale and downscale pH changes and the findings will be the basis for a separate paper.

**Carboxyl Ionization.** Whitesides<sup>29</sup> studied the acid–base behavior of carboxylic acid groups covalently attached to the surface of polyethylene. Contact angle studies suggested that the ionization begins at pH 6, reaches 50% ionization at pH 7.5, and is fully ionized at pH 11. Below pH 5, the data suggested that all groups were in the carboxyl form. However, Marlow<sup>19</sup> carried out a theoretical and experimental investigation of a

single acid site (carboxyl) polymer colloid latex and showed, from the pH dependence of microelectrophoresis, that ionization was complete above pH 8; a substantial negative mobility persisted well below pH 5 and did not approach zero until very close to pH 2, where a small positive mobility appeared in 10 mM KCl. Rowell<sup>30</sup> reported similar measurements on a different carboxylic latex and also found a small positive mobility near pH 2 in KCl at  $p\lambda$  4. Borkovec<sup>31</sup> reported electrophoresis measurements on carboxyl latex particles that gave a small positive mobility at pH 3 in 100 mM KCl. There was also substantial negative mobility below pH 5, and the data did not approach zero until pH 3. The electrophoretic mobility results for carboxylic functional latexes are consistent with our data on the T-cells. The studies also suggest that the microelectrophoretic method is a much more sensitive measurement of surface charge than the earlier indirect approach using contact angle measurements.

(28) Ahimou, F.; Denis, F. A.; Touhami, A.; Dufrene, Y. F. *Langmuir* **2002**, *18*, 9937.

(29) Holmes-Farley, S. R.; Reamey, R. H.; McCarthy, T. J.; Deutch, J.; Whitesides, G. M. *Langmuir* **1985**, *1*, 725.

(30) Prescott, J. H.; Shiau, S.-j.; Rowell, R. L. *Langmuir* **1993**, *9*, 2071.

(31) Behrens, S. V.; Christl, D. I.; Emmerzael, R.; Schurtenberger, P.; Borkovec, M. *Langmuir* **2000**, *16*, 2566.

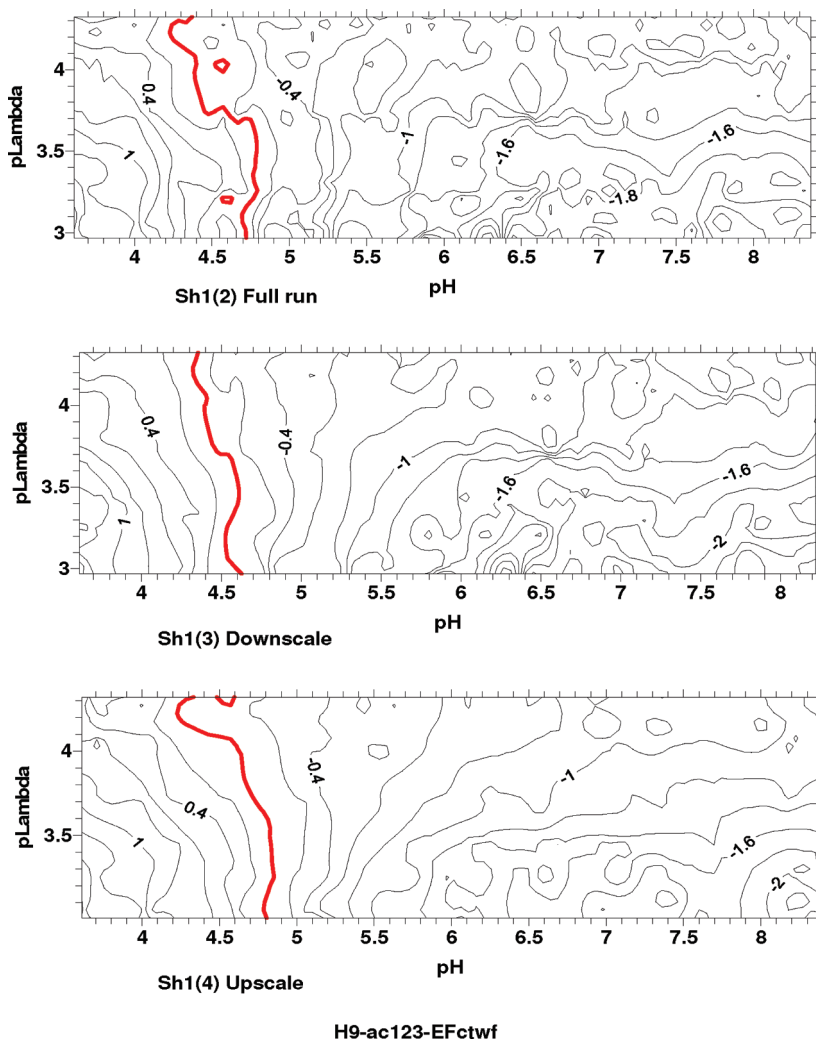


**Figure 16.** Electrophoretic fingerprints of activated H9: top, full run; middle, downscale; and bottom upsweep prepared from 18 files covering 200 mM NaCl to 5 mM NaCl.

**Interfacial Hydration.** The state of water close to an interface was not included in the DLVO theory.<sup>32</sup> However, Frens and Overbeek<sup>33,34</sup> recognized a solvation barrier present at the particle surface. Dumont and Watillon<sup>35</sup> described water structure effects as arising from an enhancement of interfacial structure by counterions resulting in a steric hydration barrier. Healy et al.<sup>36</sup> proposed a simpler, and possibly more plausible, interpretation that hydrated counterions need to be partially or completely dehydrated during interfacial molecular interactions. Butt<sup>37</sup> has reviewed studies of the interface by AFM in which the tip experiences electrostatic, van der Waals, and hydration forces when applied to a surface. He showed that, at salt concentrations above 1 M, the electrostatic repulsion can be ignored, so that the hydration force can be isolated. The hydration force has been studied extensively by Pashley and Israelachvili,<sup>38–40</sup> and the

work revealed that the repulsion depends on the type, and valence of, hydrated adsorbed cations. Pashley<sup>38</sup> further suggested that the repulsive force arose because of the work required to dehydrate the adsorbed ions. Molina-Bolivar et al.<sup>41</sup> have studied the stability of protein-covered colloidal systems in order to demonstrate the role of hydration forces in explaining the anomalous stability of lipid bilayers and other model membranes in aqueous solution.

The above is but a small selection of the vast literature studies of hydration forces, but it illustrates that results of our EF studies are consistent with their findings and that our conclusions have validity. However, 2D wireframes and LZM shifts seen in the EFs also reveal something of the nature of the dynamic changes that occur as hydrated protons in bulk solution interact to neutralize surface carboxyl groups or add charge to amino family surface groups, with consequent changes in the state of hydration at each stage. The changes in electrophoretic mobility during upscale and downscale pH sweeps reflect the different rates of the respective ionization and association that occur in the surface functional groups as a consequence of the different changes in the hydration–dehydration reactions involved.

- (32) Verwey, E. J. W.; Overbeek, J. Th. G. *Theory of the Stability of Lyophobic Colloids*; Elsevier: New York, 1948.
- (33) Frens, G.; Overbeek, J. Th. G. *J. Colloid Interface Sci.* **1971**, *36*, 286.
- (34) Overbeek, J. Th. G. *J. Colloid Interface Sci.* **1977**, *58*, 408.
- (35) Dumont, F.; Watillon, A. *Disc. Faraday Soc.* **1971**, *52*, 352.
- (36) Healy, T. W.; Homola, A.; James, R. O.; Hunter, R. J. *Faraday Discuss. Chem. Soc.* **1978**, *65*, 156.
- (37) Butt, H. J. *Biophys. J.* **1991**, *60*, 1438.
- (38) Pashley, R. M. *J. Colloid Interface Sci.* **1981**, *80*, 153.
- (39) Pashley, R. M. *J. Colloid Interface Sci.* **1981**, *83*, 531.
- (40) Pashley, R. M.; Israelachvili, J. *Colloid Interface Sci.* **1984**, *97*, 446.

- (41) Molina-Bolivar, J. A.; Galisteo-Gonzalez, F.; Hidalgo-Alvarez, R. *Phys. Rev. E* **1997**, *55*, 4522.

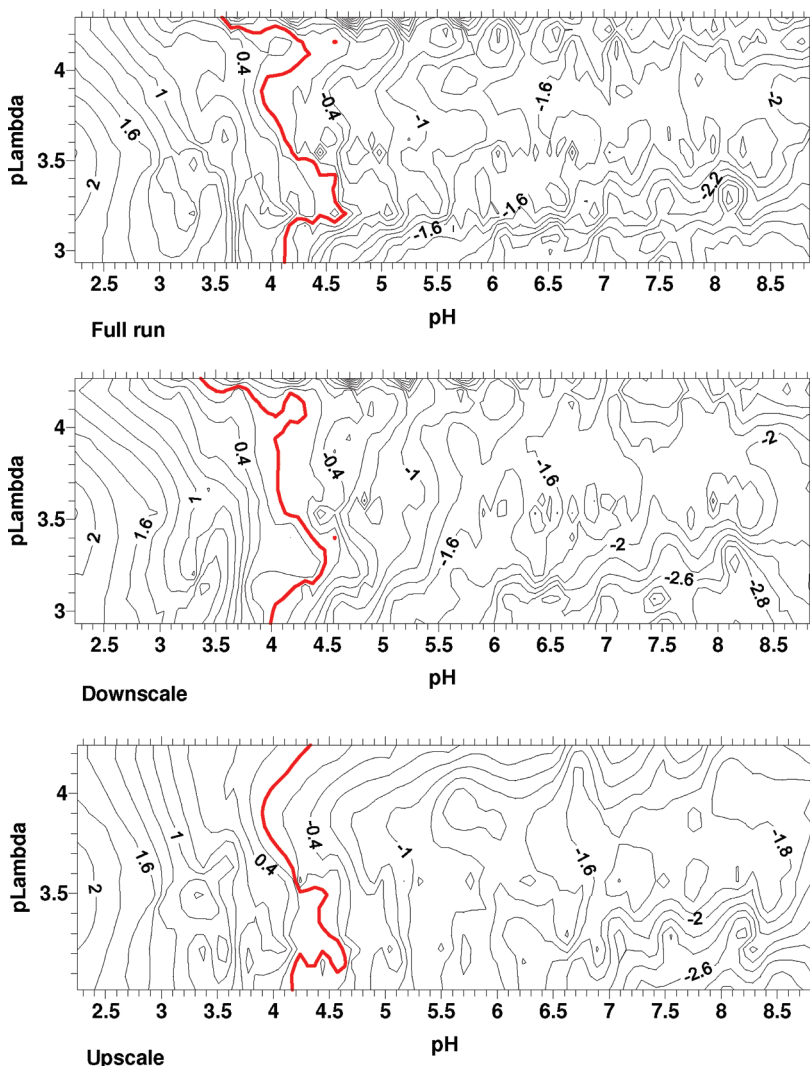


**Figure 17.** Electrophoretic fingerprints of replicating Molt 4: top, full run; middle, downscale; and bottom, upscale prepared from 21 files covering 200 mM NaCl to 5 mM NaCl.

### Conclusions

This study has generated data on the surface charge characteristics of model cellular targets for HIV-1 infection and, not unexpectedly, has raised issues that warrant further study. Work on the model (T-cell) systems has provided insight into the effects of solution pH and conductivity that can now be extended to the HIV viron itself.

- 1 The upscale and downscale pH sweeps are different. The data suggest that it is easier to protonate a protein cell surface than to deprotonate it. This may be, potentially, of biological significance and particularly relevant to HIV-1 infection, since the environment where most infections occur undergoes this protonation effect prior to transmission.
- 2 The differences in upscale and downscale pH sweeps are most pronounced at the highest salt concentration (similar to that which exists for the cells in their native state) and become less pronounced as the salt concentration is lowered. The differences are most difficult to detect at the lowest salt concentrations measured; this may arise from changes in the solvation and folding state of the surface proteins.

- 3 Characteristic ieps have been estimated for three CD+ T-cell lines, in both the replicating and highly activated states.
- 4 Characteristic LZMs have been reported for three T-cell lines in both the replicating and highly activated states. In general, LZMs for upscale EFs are shifted to higher pH than for downscale EFs.
- 5 LZMs at the highest salt concentration for all three cell lines in both the replicating and highly activated states tend to be at lower pH than the corresponding ieps.
- 6 A plot of  $p\lambda$  vs  $p[\text{NaCl}]$  has been found essential in evaluating the consistency of the electrophoretic mobility measurements at different (1:1) electrolyte concentrations.
- 7 Electrophoretic mobility measurements as a function of pH have, for the first time, been shown to reflect different rates of the respective ionization and association that occur in the surface functional groups as a consequence of the different changes in the hydration-dehydration reaction involved.

The electric double layer of living biological cells differs from ordinary organic/inorganic dispersed particles in that, in addition

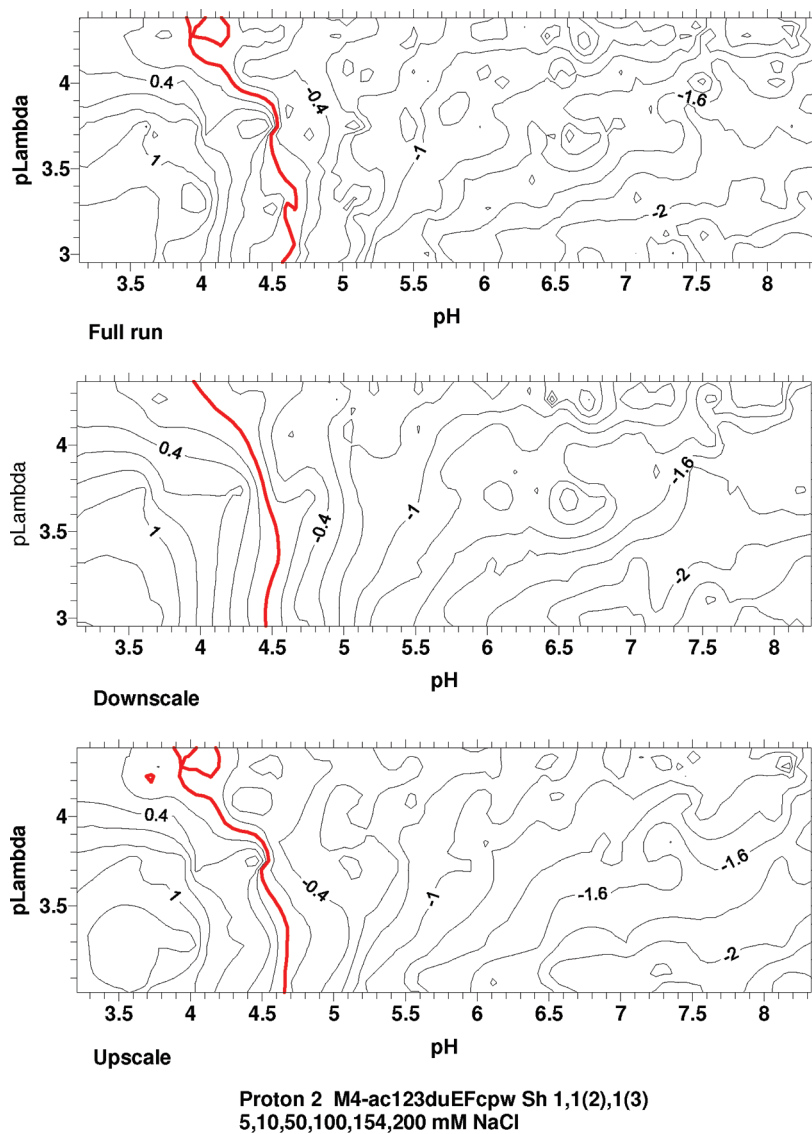


**Figure 18.** Electrophoretic fingerprints of activated Molt 4: top, full run; middle, downsweep; and bottom, upsweep prepared from 15 files covering 200 mM NaCl to 5 mM NaCl.

**Table 1. Isoelectric Points of CD4+ T-Cells**

cell line	unactivated		sample	activated	
	downscale	upscale		downscale	upscale
H9	4.45	4.2		4.6	4.8
C8166	4.6	4.8	ac1	4.1	4.5
			ac2	4.5	5.3
			ac3	4.5	5.2
Molt 4	4.0	4.2		4.4	4.5

to the usual mechanisms of formation (dissociation of surface groups and/or adsorption of ionogenic moieties), two other factors play a role vis their nonequilibrium state and the presence of a highly conducting intracellular closed volume separated from the bulk solution by a slightly conducting lipid membrane that resulted in a transmembrane potential.<sup>42,43</sup> This will undoubtedly be affected by the ionic strength and may give rise to some of the observed variability seen in the up and down sweeps. It also points

to the fact that simple electrostatics are likely insufficient to explain all the results.

We also wish to reiterate that the current data are obtained using *model* cells and may not fully represent *in vivo* realities. The immortalized cell lines used in the current study are, inherently, at a low to moderate level of activation as they are constantly actively dividing. While there are ways to slow down cell division, this would not alter anything fundamentally; measurements on such cells would likely mirror the EFs and 2D wireframes presented here. To measure true resting cells, primary cells that have been isolated and untreated can be compared to activation of these same cells and would reflect a state in which they would be more functionally developed with respect to viral clearance. Either way, resting or activated, primary cells are vulnerable to infection. Work is now in progress using nonproliferating primary cells; we might expect a significant difference from the target cells used in the current studies.

**Acknowledgment.** The work was supported by a grant from the International Partnership for Microbicides, Silver Spring, MD 20910, USA.

(42) Redman, K.; Burmeister, J.; Jensen, H. *Acta Biol. Med. Ger.* **1974**, *33*, 187.  
(43) Dukhin, A. S. *Colloids Surf., A* **1993**, *73*, 29.